Sea Level Rise and Urban Infrastructure

By ALLAN HSIAO*

How exposed are cities to the threat of sea level rise? I quantify this exposure for cities worldwide with a focus on urban infrastructure. I document three facts. First, Asian cities are the most exposed cities in the world. Second, poorer cities and neighborhoods are less exposed than richer cities and neighborhoods. Third, exposure accelerates as sea level rise passes 1.5 meters.

I. Data

I compile global data on sea level rise (SLR) and urban infrastructure at a resolution of 30 meters (m). These granular data capture rich, within-city heterogeneity in the incidence of SLR and the distribution of infrastructure.

A. Sea level rise

The Intergovernmental Panel on Climate Change (IPCC) projects 0.44 to 0.76 m of global mean SLR by 2100 under an intermediate emissions scenario (Fox-Kemper et al., 2021). Projections rise to 0.63 to 1.60 m under higher emissions, with a large range reflecting deep uncertainty over potential ice-sheet instability and other physical processes. Moreover, for many coastal cities, land subsidence leads to a sinking coastline that greatly accelerates SLR in relative terms. The worst-affected cities – largely concentrated in Asia – are sinking between 5 and 15 millimeters (mm) per year (Tay et al., 2022).

I use elevation data and a simple physical model to assess inundation under SLR of 0 to 5 m in 0.1-m increments. I obtain global elevation data at 30-m resolution from the DeltaDTM Global Coastal Digital Terrain Model, which isolates the bare-earth surface of coastal areas (Pronk et al., 2024). The data cover the Low Elevation Coastal Zone (LECZ), defined as low-lying coastal areas with elevation less than 10 m above mean sea level. These data remove elevation bias from the Copernicus GLO-30 Digital Surface Model, which does not separate forests and buildings from bare-earth surface. The Copernicus data derive from satellite measurements taken on the TanDEM-X mission from 2011 to 2015, and they include a water body mask that distinguishes land from ocean, lakes, and rivers.

For a cell i, I thus observe elevation e_i and dummy o_i, which records whether the cell is ocean. I model inundation $n_i(s)$ under SLR scenario s by applying the principle of hydrologic connectivity (Bracken et al., 2013). I mark current ocean cells as inundated.

$$n_i(s) = o_i$$

Then I simulate the path of the ocean to identify cells under direct threat. I mark cells as inundated if they are (a) adjacent to an inundated cell and (b) below sea level.

$$n_i'(s) = a_i(s) \cdot b_i(s)$$

These conditions are given by

$$a_i(s) = \mathbb{1}\left[\sum_j a_{ij} n_j(s) > 0\right],$$
$$b_i(s) = \mathbb{1}[e_i < s],$$

where a_{ij} records whether cells i and j are adjacent, including diagonally. I repeat until I identify all inundated cells. I assume no inundation up to 5 m of SLR if a cell is not in the LECZ or if it is more than 500 km from the ocean.

The model captures permanent risk under SLR. First, it does not capture temporary risk from tides and storm surges. Evaluating such risk requires more sophisticated hydrological modeling that incorporates factors like runoff responses, soil characteristics, and land use. Permanent risk is simpler because land in the ocean's direct path is at risk whether the soil along that path is porous or not. Second, for a particular city, inundation risk arises from global mean SLR in combination with local land sub-
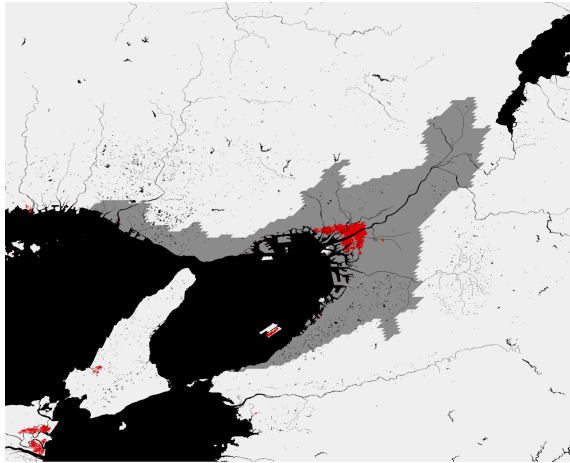
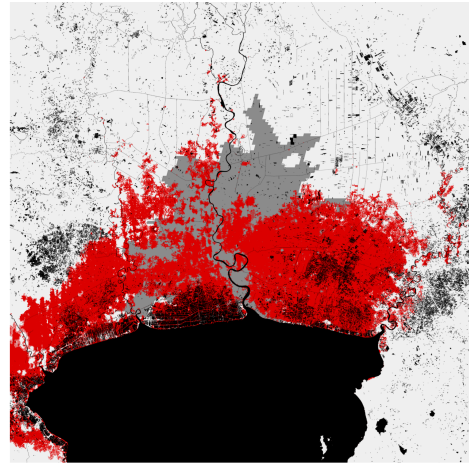*A. Osaka (1 m SLR)*   *B. Bangkok (2 m SLR)*

FIGURE 1. INUNDATION UNDER SLR

Note: Each map has four colors. Black is ocean, rivers, and lakes, dark gray is land within the urban boundary, and light gray is other land. Red is simulated inundation under SLR of 1 m in the left figure and 2 m in the right figure.

sidence. Fast-subsiding cities will experience each SLR scenario before slow-subsiding cities do. Third, the model does not capture present or future adaptation. Many Dutch cities lie below sea level, but the Netherlands has adapted with flood defense at national scale. The model identifies inundation risk and not inundation itself.

Figure 1 illustrates for two of the most exposed cities in the world. Under SLR of 1 m, inundation risk for Osaka is concentrated at the mouth of the Yodo river delta. Areas farther upstream remain relatively exposed, as does much of the rest of Osaka Bay. Under SLR of 2 m, much of Bangkok is at risk of inundation. The risk is not restricted to the riverbanks of the Chao Phraya and instead extends throughout the Bay of Bangkok.

B. Urban infrastructure

I obtain urban boundaries at 1-km resolution from the Global Human Settlement Layer Urban Center Database (GHS-UCDB) by Uhl et al. (2024). These boundaries delineate urban clusters, which I refer to as "cities," of contiguous cells with population densities of at least 1,500 per km^2 and total populations of at least 50,000 in 2025. Granular population data are derived from build-up surface data, as extracted from Landsat and Sentinel-2 satellite imagery. In this sample, the most populous cities are the

Guangzhou, Jakarta, and Dhaka metropolitan areas with populations of 43.0, 40.5, and 37.3 million. The largest cities are Dhaka, Guangzhou, and Tokyo with land areas of 6,611, 6,454, and 5,165 km^2. The average city has a population of 0.3 million and an area of 57 km^2. I refine these boundaries with the 30-m resolution water body mask by dropping ocean, lake, and river cells.

For each city, I compile geocoded data on education, health, and transport infrastucture. Education and health data from OpenStreetMap record schools, kindergartens, colleges, universities, hospitals, clinics, doctor practices, dentist practices, and pharmacies in 2024. "Schools" include primary, middle, and high schools but do not distinguish among them. Transport data from the Global Roads Inventory Project (GRIP) records highways, primary, secondary, and tertiary roads with the most recent temporal coverage available when assembled in 2018.

I assess distributional effects with income data. I study heterogeneity across cities with country-level GDP data for 2020 from GHS-UCDB. I define higher-income cities as those in countries with above-median GDP relative to other countries. I study heterogeneity within cities by proxying with cell-level night light intensity data for 2023 from Earth Observation Group (EOG). I define higher-income neighborhoods as cells with above-median night light intensity relative to other cells in the same city.

TABLE 1—PERCENT OF INFRASTRUCTURE EXPOSED

Rank	SLR of 1 m		SLR of 2 m		SLR of 3 m	
	City	%	City	%	City	%
1	Osaka	4.8	Bangkok	55.5	Bangkok	94.4
2	Jakarta	2.2	Shanghai	19.0	Shanghai	80.2
3	Tokyo	2.2	Manila	11.8	Suzhou	31.3
4	Lagos	1.7	Osaka	9.9	Lagos	25.7
5	Mumbai	1.1	Jakarta	9.5	Manila	21.3
6	Manila	1.0	Lagos	9.0	Ho Chi Minh City	20.9
7	New York City	0.4	Tokyo	5.4	Kolkata	20.1
8	Suzhou	0.2	Ho Chi Minh City	4.0	Jakarta	16.3
9	Bangkok	0.2	Kolkata	3.8	Osaka	15.7
10	Shanghai	0.2	New York City	2.7	Guangzhou	12.5

Note: The table lists the ten most exposed cities under SLR of 1, 2, and 3 m. For each SLR scenario, I compute the percentage of education, health, and transport infrastructure that is exposed to inundation. Education infrastructure is schools, health infrastructure is hospitals and clinics, and transport infrastructure is highways and primary roads. I compute education, health, and transport percentages separately, then I take the average to obtain a single infrastructure percentage.

These data are measured at 450-m resolution and derive from Visible Infrared Imaging Radiometer Suite (VIIRS) satellite measurements. I downscale the data to 30-m resolution.

II. Exposure

I assess the exposure of cities to future SLR. In particular, I compute the percentage of land and infrastructure at risk of inundation under SLR of 0 to 5 m.

A. Asian cities are highly exposed

For each city, I compute the percentage of education, health, and transport infrastructure inundated under each SLR scenario. Education infrastructure is schools, health is hospitals and clinics, and transport is highways and primary roads. The schools data pool primary, middle, and high schools. I pool hospitals and clinics: I simply count the number of inundated facilities and divide by the total number of facilities. I similarly pool highways and primary roads. I define infrastructure exposure as the equal-weighted average of these education, health, and transport percentages.

Table 1 presents the 10 most exposed cities under SLR of 1, 2, and 3 m. Asian cities dominate each list. Under SLR of 1 m, 4.8% of Osaka's infrastructure is at risk of inundation –

twice as high as Jakarta and Tokyo, which follow. Lagos and New York City are the only non-Asian cities on the list. Under SLR of 2 m, Bangkok and Shanghai rise to the top of the list. Bangkok in particular faces the risk of widespread inundation. Manila also rises, and Lagos and New York City are still the only non-Asian cities. Under SLR of 3 m, Bangkok and Shanghai continue to top the list. Nearly all of Bangkok's infrastructure is at risk of inundation. Shanghai is also severely exposed at 80.2%, and Chinese cities occupy 3 of the top 10 positions. Lagos is the only non-Asian city that remains, but it too is highly exposed at 25.7%.

B. Lower-income places are less exposed

I consider distributional effects both across and within cities. I study across-city heterogeneity by aggregating over cities according to country-level GDP. For land, I calculate the at-risk and total area for each of my cities of interest. For cities c, at-risk areas n_c, total areas N_c, and population densities p_c, this aggregate exposure is

$$\bar{e} = \frac{\sum_c n_c p_c}{\sum_c N_c p_c}.$$

I repeat for education infrastructure by counting schools, for health infrastructure by counting hospitals and clinics, and for transport infrastructure by counting kilometers of highways
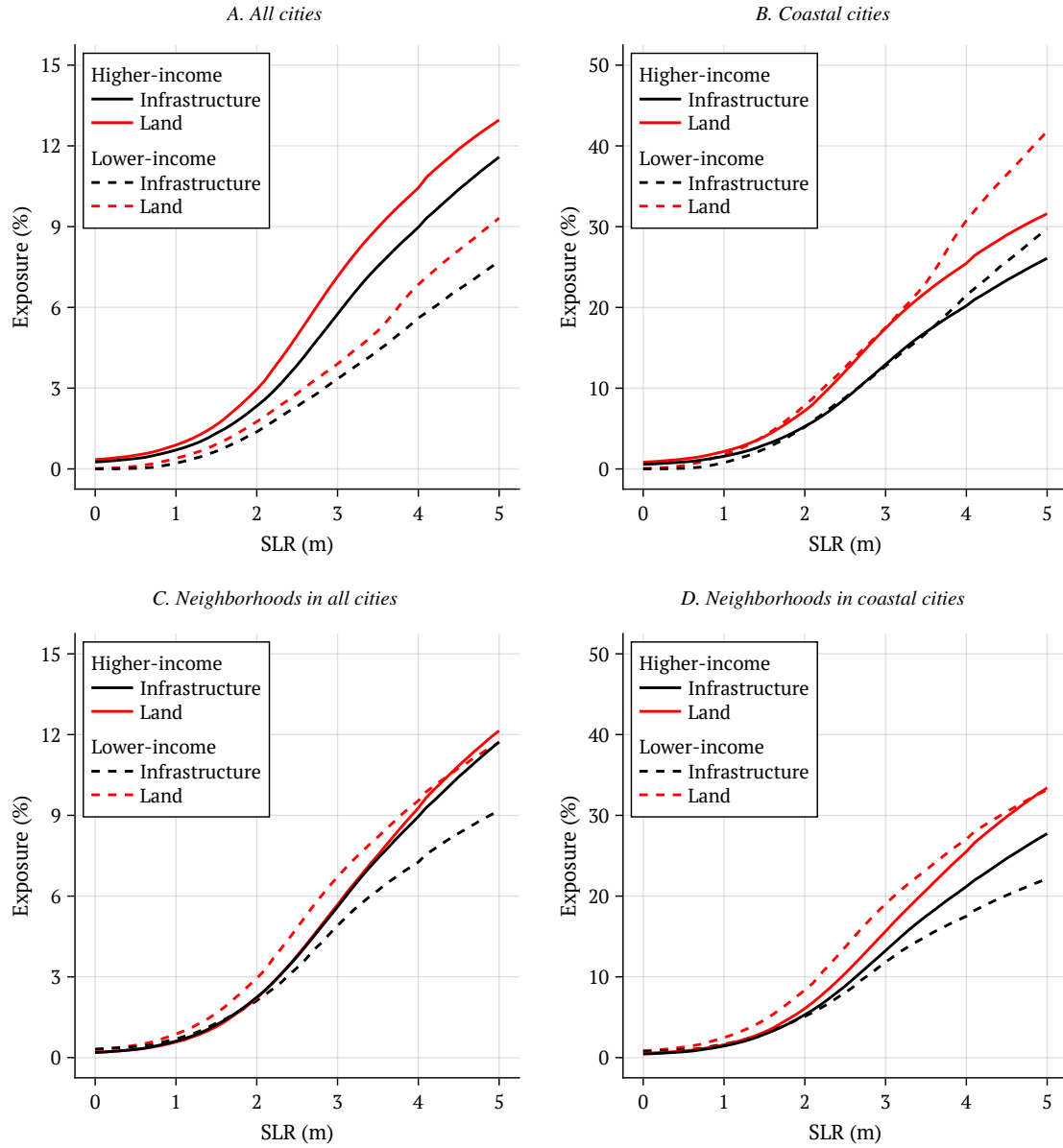
FIGURE 2. HETEROGENEITY IN INCOME

Note: For each figure, the *y*-axis shows the percentage of land or infrastucture exposed to inundation under SLR. The *x*-axis shows SLR scenarios of increasing severity. Land is land area within each urban boundary. Infrastructure is an equal-weighted average of education, health, and transport infrastructure. Education infrastructure is schools, health is hospitals and clinics, and transport is highways and primary roads. In figures A and B, lower-income cities are cities in countries with below-median GDP relative to other countries, while higher-income cities are above-median. In figures C and D, lower-income neighborhoods are cells with below-median night light intensity relative to other cells in the same city, while higher-income neighborhoods are above-median. Figures A and C include all 11,422 cities. Figures B and D are restricted to the 2,087 coastal cities that face some degree of land inundation risk under SLR of 5 m. The *y*-axis is smaller for figures A and C than it is for figures B and D.

and primary roads. I average these three measures to obtain an overall measure for infrastructure. I similarly study within-city heterogeneity by aggregating over neighborhoods according to cell-level night light intensity.

Figure 2A shows that lower-income cities have less exposure than higher-income cities for both land and instructure. At all levels of SLR, higher-income land exposure exceeeds lower-income land exposure, and the same holds for

infrastructure. The reason is that higher-income cities are more likely to be coastal. Figure 2B conditions on coastal cities, which I define as cities with any inundated land under SLR of 5 m. I identify 2,087 such cities. Lower-income cities remain less or similarly exposed under low and medium levels of SLR. But lower-income exposure accelerates and surpasses higher-income exposure after 3.5 m of SLR.

Figure 2C shows that lower-income neighborhoods have lower infrastructure exposure than higher-income neighborhoods, despite having higher land exposure. The reason is that infrastructure is relatively well-placed in lower-income neighborhoods. Infrastructure in higher-income neighborhoods is spread more evenly over space, and so infrastructure exposure aligns with land exposure. Infrastructure in lower-income neighborhoods is concentrated on relatively safe land, and so infrastructure exposure does not rise as quickly as land exposure. Figure 2D shows that this pattern also holds for coastal cities, where the gap between lower-income infrastructure and land exposure is even larger. The same is true to a lesser extent for higher-income neighborhoods.

C. Inundation risk is modest for SLR below 1.5 m

Each curve in figure 2 features a similar inflection point. Inundation risk rises at a modest pace with SLR of 1.5 m or less. Moreover, in absolute terms, inundation risk is modest below this level. Under SLR of 1 m, inundation risk is roughly 1% for all cities and 2% for coastal cities. Cities should seek to limit local land subsidence, as global mean SLR is projected to remain within this range. Inundation risk rises more rapidly with SLR at higher levels, with roughly 10% exposure for all cities and 30% for coastal cities under SLR of 5 m.

III. Implications

I assess the threat of sea level rise for cities worldwide, and I document meaningful inundation risk for both land and critical infrastructure. How can cities adapt? How can governments help? These are the key questions facing the people and politicians of our coastal cities. Rapid land subsidence has placed Jakarta at the forefront of navigating this threat. It provides an important setting for studying the challenges of urban adaptation (Hsiao, 2023) and the implications for urban inequality (Hsiao, 2024).

REFERENCES

Bracken, Louise, John Wainwright, Geneviève Ali, Dörthe Tetzlaff, Mark Smith, Sim Reaney, and André Roy. 2013. "Concepts of hydrological connectivity: Research approaches, pathways and future agendas." *Earth-Science Reviews*, 119: 17–34.

Fox-Kemper, Baylor, Helene Hewitt, Cunde Xiao, et al. 2021. "Ocean, Cryosphere and Sea Level Change." In *Climate Change 2021: The Physical Science Basis. Contribution of Working Group I to the Sixth Assessment Report of the Intergovernmental Panel on Climate Change*. Chapter 9, 1211–1362. Cambridge University Press.

Hsiao, Allan. 2023. "Sea Level Rise and Urban Adaptation in Jakarta."

Hsiao, Allan. 2024. "Sea Level Rise and Urban Inequality." *AEA Papers and Proceedings*, 114: 47–51.

Pronk, Maarten, Aljosja Hooijer, Dirk Eilander, Arjen Haag, Tjalling de Jong, Michalis Vousdoukas, Ronald Vernimmen, Hugo Ledoux, and Marieke Eleveld. 2024. "DeltaDTM: A Global Coastal Digital Terrain Model." *Scientific Data*, 11: 273.

Tay, Cheryl, Eric Lindsey, Shi Tong Chin, Jamie McCaughey, David Bekaert, Michele Nguyen, Hook Hua, Gerald Manipon, Mohammed Karim, Benjamin Horton, Tanghua Li, and Emma Hill. 2022. "Sea-Level Rise from Land Subsidence in Major Coastal Cities." *Nature Sustainability*, 5(12): 1049–1057.

Uhl, Johannes, Martino Pesaresi, Luca Maffenini, Patrizia Sulis, Monica Crippa, Diego Guizzardi, Enrico Pisoni, Claudio Belis, Duarte Oom, Alfredo Branco, Dennis Mwaniki, Edwin Kochulem, Daniel Githira, Alessandra Carioli, Daniele Ehrlich, Pierpaolo Tommasi, Thomas Kemper, and Lewis Dijkstra. 2024. "Stats in the City GHSL Urban Centre Database 2025."